



Dipolar and V-shaped structures incorporating methylenepyran and diazine fragments

Sylvain Achelle ^{a,*}, Samia Kahlal ^b, Jean-Yves Saillard ^b, Nolwenn Cabon ^a, Bertrand Caro ^a, Françoise Robin-le Guen ^a

^a Institut des Sciences Chimiques de Rennes UMR CNRS 6226, IUT de Lannion, rue Edouard Branly, BP 30219, F22302 Lannion Cedex, France

^b Institut des Sciences Chimiques de Rennes UMR CNRS 6226, Campus de Beaulieu, 263 av. du Général Leclerc, 35042 Rennes, France

ARTICLE INFO

Article history:

Received 14 January 2014

Received in revised form 17 February 2014

Accepted 24 February 2014

Available online 6 March 2014

ABSTRACT

Thirteen novel dipolar and V-shaped chromophores with pyranlidene electron-donating part, diazine electron-withdrawing part and various π -linkers were synthesized. The extent of intramolecular charge transfer, structure-property relationships and optical properties were further investigated by UV/Vis absorption, electrochemistry, and DFT calculations.

© 2014 Elsevier Ltd. All rights reserved.

Keywords:

Methylenepyran

Diazines

Push–pull

DFT calculations

Dyes

1. Introduction

In the last several years, dipolar molecules ($D-\pi-A$) also called push–pull molecules bearing electron donors and acceptors linked by a π -conjugated core have been subject to intensive investigation due to their prospective application as efficient materials in organic electronics and optoelectronics.¹ Intramolecular charge transfer (ICT) derives from the push-pull structure and such molecules have found applications as fluorescent dyes,² component for light emitting devices,³ solar cells materials⁴ and second and third order non-linear optical (NLO) materials.⁵ V-shaped $D-\pi-A-\pi-D$ design is also typical of light emitting and third order NLO chromophores. The chromophore polarizability depends mainly on its chemical structure in particular on the length on the π -conjugated spacer and the electronic nature of the attached donors and acceptors.⁶ The ability of the π -conjugated oligomers as chromophores and electrophores is related to the intramolecular delocalization of π -electrons along the molecular chain.

γ -Methylenepyrans are versatile six atom heterocycles with a proaromatic electron-donor character. It is well-known that chromophores incorporating aromatic subunits display lower β values than the corresponding polyenes of the same conjugation

length, since their ground states are usually dominated by neutral, aromatic forms that lose resonance energy on charge separation.⁷ One way to overcome this drawback consists in incorporating a fragment whose aromaticity will increase upon charge transfer. In this context, γ -methylenepyran leading to aromatic pyrylium when internal charge transfer occurs are particularly attracting as donor part in push-pull structures. The use of this fragment in the structure of NLO chromophores has been already described in the literature.⁸ Moreover, π -conjugated structures incorporating γ -methylenepyran building blocks have been described as interesting redox systems.⁹

Diazines are six-membered aromatics with two nitrogen atoms. Three different structures can be distinguished according to the relative position of the nitrogen atoms: pyridazine (1,2-diazine), pyrimidine (1,3-diazine) and pyrazine (1,4-diazine). Diazines are building block of choice for the incorporation in π -conjugated materials either as electron-accepting part or as part of the π -conjugated backbone.¹⁰ 4,6-Diarylvinylpyrimidines is an important class for third order NLO chromophore and fluorophores¹¹ and numerous pyrimidine chromophores have found sensing applications.¹² A large variety of π -conjugated materials bearing pyrazine has been also described. In particular 2,3-dicyanopyrazine derivatives exhibit intense fluorescence and second-order NLO properties.¹³ Quinoxaline (benzopyrazine) derivatives have been employed in dye sensitized solar cells and in organic light emitting diodes.¹⁴ Even if less numerous, some examples of π -conjugated

* Corresponding author. Tel.: +33 (0)2 96 46 94 48; fax: +33 (0)2 96 46 93 54; e-mail address: sylvain.achelle@univ-rennes1.fr (S. Achelle).

pyridazine structures with interesting electro-optical properties have been also described.¹⁵

Recently we have described the NLO properties of two pyrimidine γ -methyleneypyran derivatives (Fig. 1).¹⁶ The aim of the present article is, with the help of electrochemical, optical and computational studies, to describe the synthesis and the ICT of a series of push-pull and V-shaped structures with an extended π -conjugated core incorporating γ -methyleneypyran as electron-donating parts and various diazine rings as electron-attracting groups.

boiling aqueous 5 M NaOH using Aliquat® 336 as a phase-transfer catalyst followed by deprotection of the acetal group in acidic media leading to compounds **9** according to the procedure initially described by Vanden Eynde and co-workers.¹⁸ The second step consists in a Wittig reaction between aldehyde **9** and 2,6-diphenyl-4H-pyran-4-yl triphenylphosphonium tetrafluoroborate salt¹⁹ leading to derivatives **10** (Scheme 4).²⁰

The same procedure has been employed with 4-methyl-2,6-dipyridin-2-yl-pyrimidine²¹ affording compound **12** (Scheme 5).

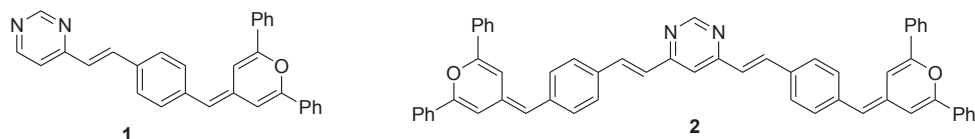
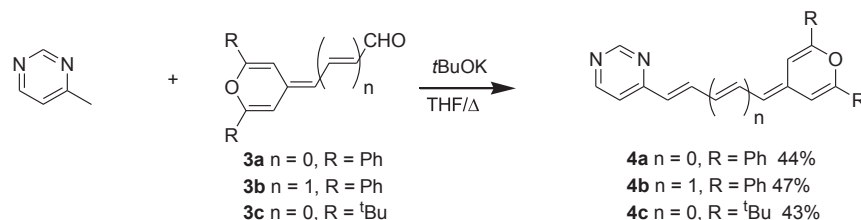


Fig. 1. Structures of compounds **1** and **2**.

2. Results and discussion

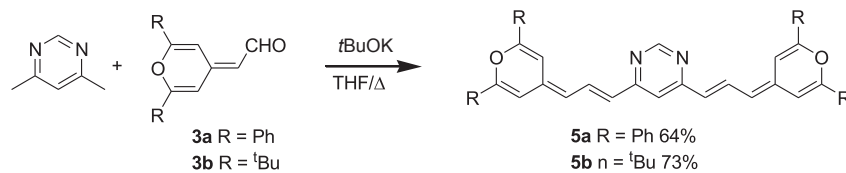
2.1. Synthesis

The main method for the synthesis of (*E*)-vinylidiazines consists in a condensation reaction between methyldiazine and aldehyde.¹⁷ The push-pull compounds **4** were obtained in moderate yields by condensation of methyleneypyran aldehydes **3** and 4-methylpyrimidine with potassium *tert*-butoxide in refluxing THF (Scheme 1).



Scheme 1. Synthesis of compounds **4**.

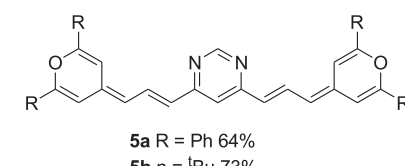
The same procedure was employed to synthesize V-shaped compounds **5** from 4,6-dimethylpyrimidine (Scheme 2) and to obtain push-pull structure with pyrazine (**6**), quinoxaline (**7**) and pyridazine (**8**) attracting part (Scheme 3). Yields obtained (43–51%) are in the same range as for pyrimidine derivatives.



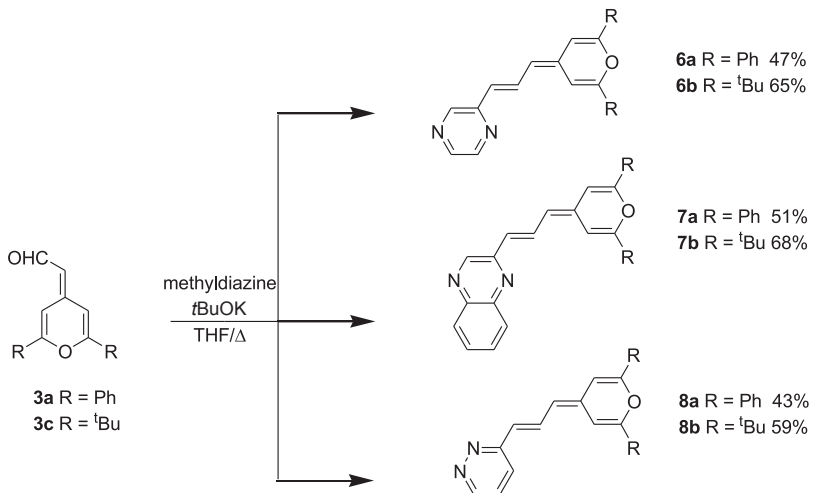
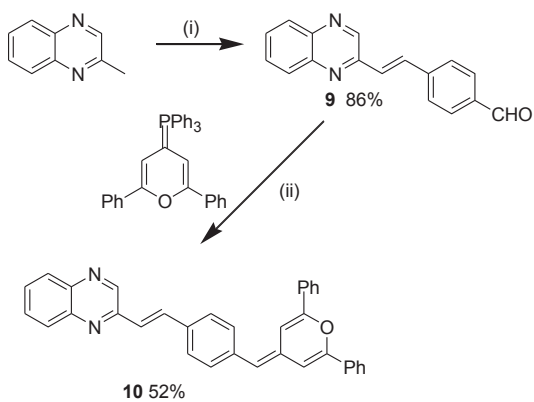
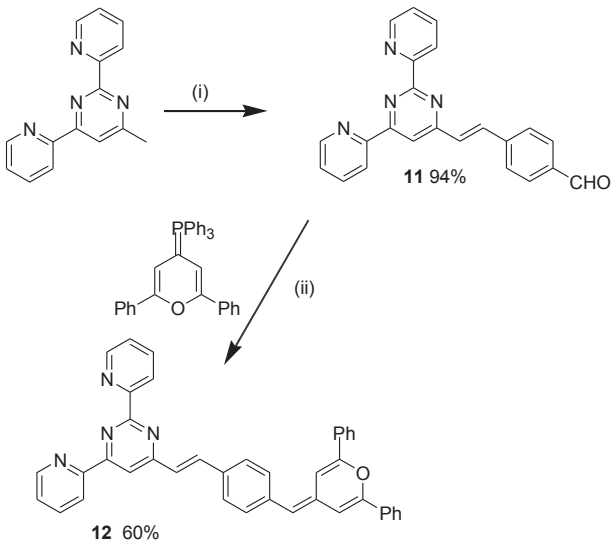
Scheme 2. Synthesis of compounds **5**.

In order to study the influence of a phenyl ring in the π -conjugated bridge between the diazine electron-attracting part and the methyleneypyran electron-donating part, a second family of compounds, similar to the structure **1** was designed. The compound **10** was obtained in two steps from 2-methylquinoxaline (Scheme 4). The first step consists in a condensation reaction between 2-methylquinoxaline and 4-(diethoxymethyl)benzaldehyde in

(acceptor), the so-called bond length alternation (BLA) depends on the strength of the acceptor donor. As a consequence, the difference ΔJ between the coupling constant $^3J_{\text{H,H}}$ of concomitant C–C bonds ranges from 6.5 Hz for unconjugated molecules to 0 Hz for molecules in which all the C–C bond lengths are equal (cyanine limit). As



shown in Table 1, calculated ΔJ values for the compounds **4**–**8** are in the 1.75 and 3 Hz range, indicating an important ICT in the molecules. The lowest ΔJ are obtained for pyrimidines derivatives **4**, which is in accordance with the fact that the pyrimidine ring is a better attracting group than the pyrazine, quinoxaline and pyridazine rings.^{2b} However, the values are higher than those found for Fisher type methyleneypyran carbene complexes^{8b} or

**Scheme 3.** Synthesis of compounds **6–8**.**Scheme 4.** (i) 4-(diethoxymethyl)-benzaldehyde, aliquat 336, 5 M NaOH aq., 15 h, Δ then HCl, acetone, 5 min room temperature (ii) Phosphorane obtained in situ from the corresponding phosphonium salt (BF_4^-) by $n\text{BuLi}$ (THF, 15 min -78°C) 30 min -78°C (30 min) then room temperature (2 h).**Scheme 5.** (i) 4-(Diethoxymethyl)-benzaldehyde, aliquat 336, 5 M NaOH aq., 15 h, Δ then HCl, acetone, 5 min room temperature (ii) phosphorane obtained in situ from the corresponding phosphonium salt (BF_4^-) by $n\text{BuLi}$ (THF, 15 min -78°C) 30 min -78°C (30 min) then room temperature (2 h).**Table 1**
¹H NMR spectroscopic data for compounds **4–8**

	4a	4b	4c	5a	5b	6a	6b	7a	7b	8a	8b
ΔJ (Hz) ^a	2	1.75	2	2.5	2.4	2.7	3	2.7	3	3	3

^a ΔJ values: average difference in $J_{\text{H},\text{H}}$ values across adjacent C=C and C–C bonds.

methylene pyrans bearing strong organic acceptor^{8d} groups with alkene chain spacer of similar length ($-0.6 < \Delta J < 1$ Hz). The degree of acceptor strength of the nitrogen heterocycles is also attainable from the NMR chemical shift values of the 3H and 5H protons of the pyran ring. These values were previously used as a criterion for the degree of pyrylium character. Increasing this character in the ground state, tends to shift the hydrogen signal to downfield. Thus by comparison of the observed 3H and 5H chemical shift values of compounds **4a–8a** (δ 3H $< \delta$ 3H < 7.10 ppm, δ 4.43 ppm $< \delta$ 5H < 6.47 ppm), **4b–8b** (δ 3H $< \delta$ 3H < 6.24 ppm, δ 5.64 ppm $< \delta$ 5H < 5.70 ppm) with those, more deshielded of comparable organometallic 2,6-diphenylmethylene pyrans bearing a $\text{C}(\text{X})=\text{W}(\text{CO})_5$ acceptor group ($\text{X}=\text{OMe, SPh}$) (δ 3H > 7.40 ppm, δ 5H > 7.00 ppm)^{8b} and push–pull 2,6-ditertiobutylmethylene pyrans synthesized by Garin group (δ 3H > 6.55 ppm, δ 5H > 6.18 ppm),^{8d} it appears that the diazines derivatives **4–8** have a lower pyrylium character.

2.3. Optical properties

The UV/Vis electronic spectra of compounds **1, 2, 4–8, 10**, and **12** were recorded in dichloromethane solution and the results are given in **Table 2**. All compounds showed longest absorption wavelengths (λ_{max}) in the visible region (425–469 nm) attributed to ICT. In most of the cases, a second or even a third absorption band of higher energy is observed. When comparing the lower energy absorption band of compounds **1** and **4a** on one hand and of compounds **10** and **7** on other hand, it appears that $\lambda_{\text{abs}}(\text{4a}) > \lambda_{\text{abs}}(\text{1})$ and $\lambda_{\text{abs}}(\text{7}) > \lambda_{\text{abs}}(\text{10})$. This indicates that the compounds without a phenyl ring in the π -conjugated bridge exhibit the highest charge transfer. Di(pyridine-2-yl) derivative (**12**) exhibits a more red shifted absorption than compound **1** (535 nm vs 560 nm) probably due to the pyridine substituents that reinforce the attracting strength of the pyrimidine. The compound **4b** exhibits an absorption band of lower energy than compound **4a** (469 vs 444 nm): the increase of the π -conjugated length leads to a red shift in

Table 2
UV-visible data of the studied compounds in CH_2Cl_2

Compound ^a	λ_{abs} (nm)	ϵ (L mmol cm^{-1})	λ_{em} (nm) ^b	Stokes shift (cm^{-1}) ^c
1	435	40.9	542	4538
	250	28.0		
2	458	67.4	556	3848
	254	46.2		
4a	444	50.9	542	4072
	298	17.9		
4b	253	22.4		
	469	59.2	535	2630
4c	300	17.7		
	254	22.4		
5a	429	28.1	493	3245
5b	503	65.3	600	3214
	303	17.7		
6a	481	73.2	610	4397
	354	21.7		
6b	440	35.6	550	4545
	295	16.3		
7a	252	22.3		
	427	27.2	501	3459
7b	348	9.9		
	480	42.0	580	3592
8a	305	19.2		
	260	20.0		
8b	470	21.7	536	2620
	353	8.2		
10	427	29.8	560	5562
	292	12.3		
12	251	17.5		
	410	25.5	512	4859
10	450	51.1	612	5882
	293	39.1		
12	460	42.0	— ^d	— ^d
	343	57.1		
	282	84.3		

^a All spectra were recorded in CH_2Cl_2 solutions at room temperature at $c=1.0 \times 10^{-5}$ to 3.0×10^{-5} M for absorption and $c=1.0 \times 10^{-6}$ to 3.0×10^{-6} M for emission.

^b Excitation at the absorption band of lower energy.

^c Calculated using the wavelength of the absorption band of lower energy.

^d No fluorescence.

absorption. When comparing compounds **4a**, **6a**, **7a**, and **8a**, it appears that the quinoxaline derivative **7a** exhibits the most red shifted absorption band (480 nm). On the contrary the pyridazine derivative **8a** exhibits the most blue shifted absorption band (427 nm). A similar tendency has been observed previously.^{2b} *tert*-Butyl derivatives (**4c**, **6b**, **7b**, and **8b**) are slightly blue shifted in absorption ($\Delta\lambda=10$ –17 nm) compared to phenyl derivatives (**4a**, **6a**, **7a**, and **8a**). V-shaped compounds (**2** and **5**) exhibit red shifted absorption and higher absorption coefficient in comparison with their dipolar equivalents (**1**, **4a**, and **4b**), the red shift is more important in case of **5** than in case of **2** probably due to the more intense ICT phenomena occurring in polyene derivatives (**4** and **5**) than in phenylenevinylene derivatives (**1** and **2**). All the compounds exhibit low emission (emission quantum yield < 0.01) in the green-yellow region (493–612 nm) except for compound **12**, which is non-emissive. Relatively high Stoke shifts are observed for all those compounds (comprised between 2600 and 5882 cm^{-1}).

In previous studies, it has been demonstrated that arylvinylidiazines can be used as colorimetric and luminescent pH sensors due to the basic character of the nitrogen atoms of the diazine rings.^{2b,12b,c,21,23} Protonation of arylvinylidiazines with non-basic donor group leads to a red shift in absorption and emission, in some cases the emission is completely quenched. It has been also demonstrated that the methylenepyran part can be also protonated to form a highly emissive pyrylium.²⁴ The behavior of the compounds with or without a phenyl ring in their π -conjugated bridge is different. The changes in the UV-vis spectra of compounds **4a**–**b**,

6a, **7a**, and **8a** are illustrated in Fig. 2 and in Supplementary data. The spectra show the progressive attenuation of the absorption band for the neutral compound on increasing the concentration of acid, whereas two new red shifted bands corresponding to the monoprotonated and diprotonated species appear.

The behavior of compounds **1** and **10** is different: a blue shifted band appears progressively upon addition of trifluoroacetic acid (Fig. 3 and Supplementary data). This band corresponds to the formation of a pyrylium. Protonated species of compounds **1** and **10** exhibit a much more intense blue shifted emission band compared to the neutral derivatives ($\lambda_{\text{em}}=450$ nm, $\Phi_F=0.13$ for compound **1** and $\lambda_{\text{em}}=479$ nm, $\Phi_F=0.25$ for compound **10**).

2.4. Electrochemical properties

Compounds **4**–**8**, **10**, and **12** were analyzed by cyclic voltammetry using CH_2Cl_2 as solvent and Bu_4NBF_4 as electrolyte (Table 3). All compounds exhibit an irreversible oxidation process at positive potential value, versus the ferrocene–ferricinium couple, which correspond to the oxidation of the methylenepyran fragment, as expected.^{9b,16} Moreover, for compounds **4a**, **4b**, **5a**, **7a**, **7b**, and **10** (Fig. 4a), a quasi-reversible reduction process, involving the acceptor fragment, is observed at negative potentials. For compounds **4c**, **5b**, **6**, **8**, and **12**, it was not possible to measure the potential value of the reduction, which should lie at more negative potentials ($E_{1/2 \text{ red}} < -2$ V vs ferrocene–ferricinium). Additional oxidations were also observed for **4a/b**, **5a/b**, **6b**, **7a/b**, and **8a/b**, which probably occur from products formed after the oxidation process. For example, for **4a**, **7a**, **8a**, the ratio ($i_{\text{pox}}/\nu^{1/2}=f(V)$) remains constant for the first oxidation process but decreases for the second oxidation, suggesting an EC (Electrochemical–Chemical) process. No attempts were made to isolate these products.

On reversal scan following the first anodic wave, new waves were observed for all compounds. As previously described, this could be attributed to small amount of product resulting from the dimerization of the oxidized form.^{9b} This process remains unclear, since several C–C coupling processes may occur. We noticed that single clear reduction peak was observed for compounds bearing a 1,4-phenylene unit (**10**, **12**), respectively, at -0.84 , -0.86 V, suggesting that dimerization may take place on the exocyclic carbon of the methylenepyran fragment. This observation is consistent with the formation of a radical cation, which is transformed into a bispyrylium compound, detected on the back scan. Also, single clear reduction peak was observed for the quinoxaline compounds **7a** and **7b**, respectively, at -0.65 and -0.72 V. Whereas the reduction peak, attributed to the pyrylium center, of **10** and **12** is comparable to the analogous bispyrylium compound bearing a phenyl substituent (-0.86 V), a positive shift of the cathodic peak is observed for the dimerization compounds **7a** and **7b**.

For chromophores **4**–**8**, **10**, and **12**, the first oxidation is observed between 0.10 and 0.29 V. The electronic nature of the appended substituent ($R=\text{'Bu}$ or phenyl) of the methylenepyran core, influence the first oxidation potential only negligibly (**5a/b**, **6a/b**, **7a/b**, **8a/b**). Moreover, when comparing the compounds **4a** and **4b**, which differ by the presence of an additional vinylene linkage in **4b**, a moderate difference was found in the oxidation potential of **4a** (0.27 V) and **4b** (0.10 V). It is noticeable that no influence was observed on the reduction wave of the pyrimidine moiety. Similar trends were already observed for pyrrolopyridazine derivatives.²⁵ Finally, comparison of the potential values obtained for compounds **1** versus **4a**, **2** versus **5a** and **8a** versus **10**, which differ by the presence of the 1,4-phenylene unit, did not show effect on the oxidation or reduction potential value. From an electrochemical point of view, this means that all compounds are engaged similarly in ICT.

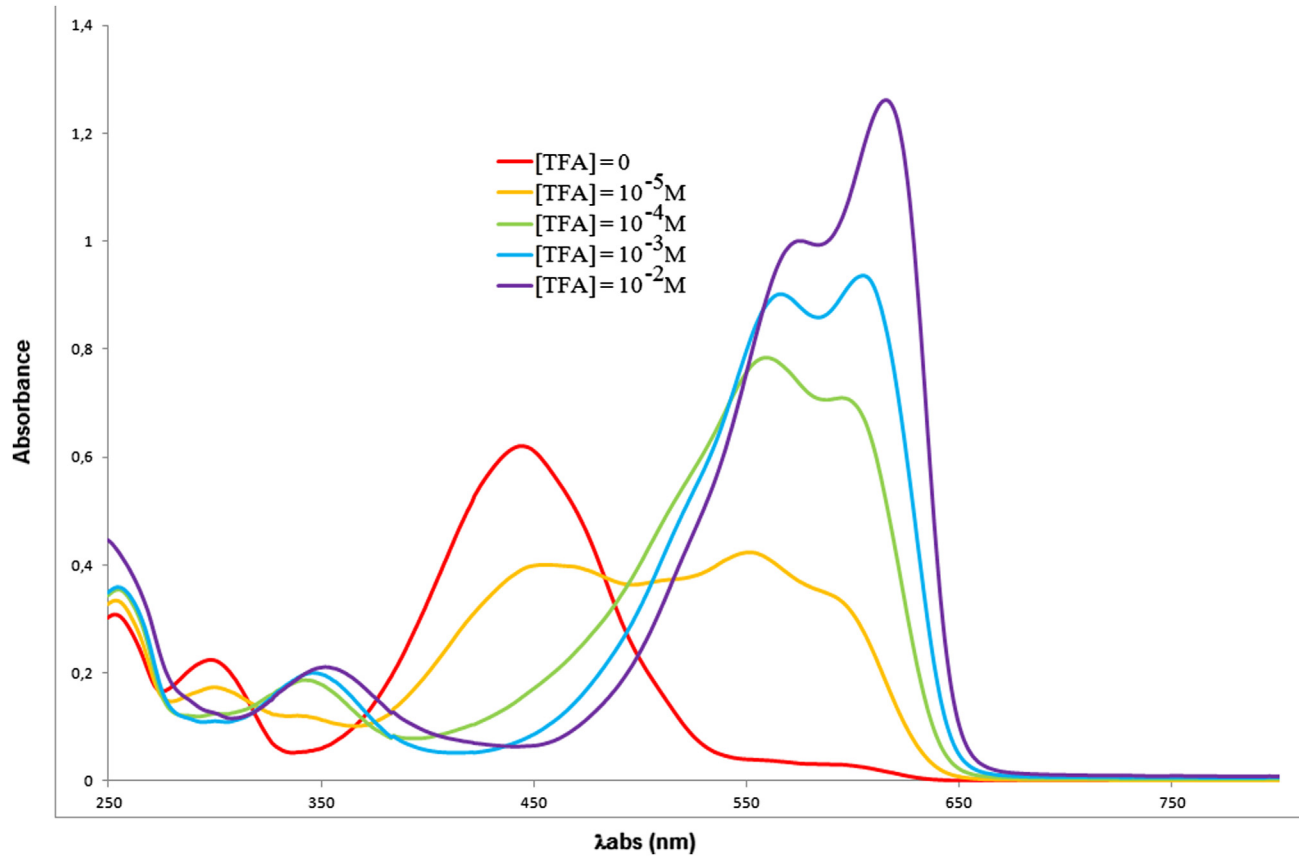


Fig. 2. UV/vis absorption change of **4a** in CH_2Cl_2 ($c=2.3 \cdot 10^{-5} \text{ M}$) with increasing TFA concentration.

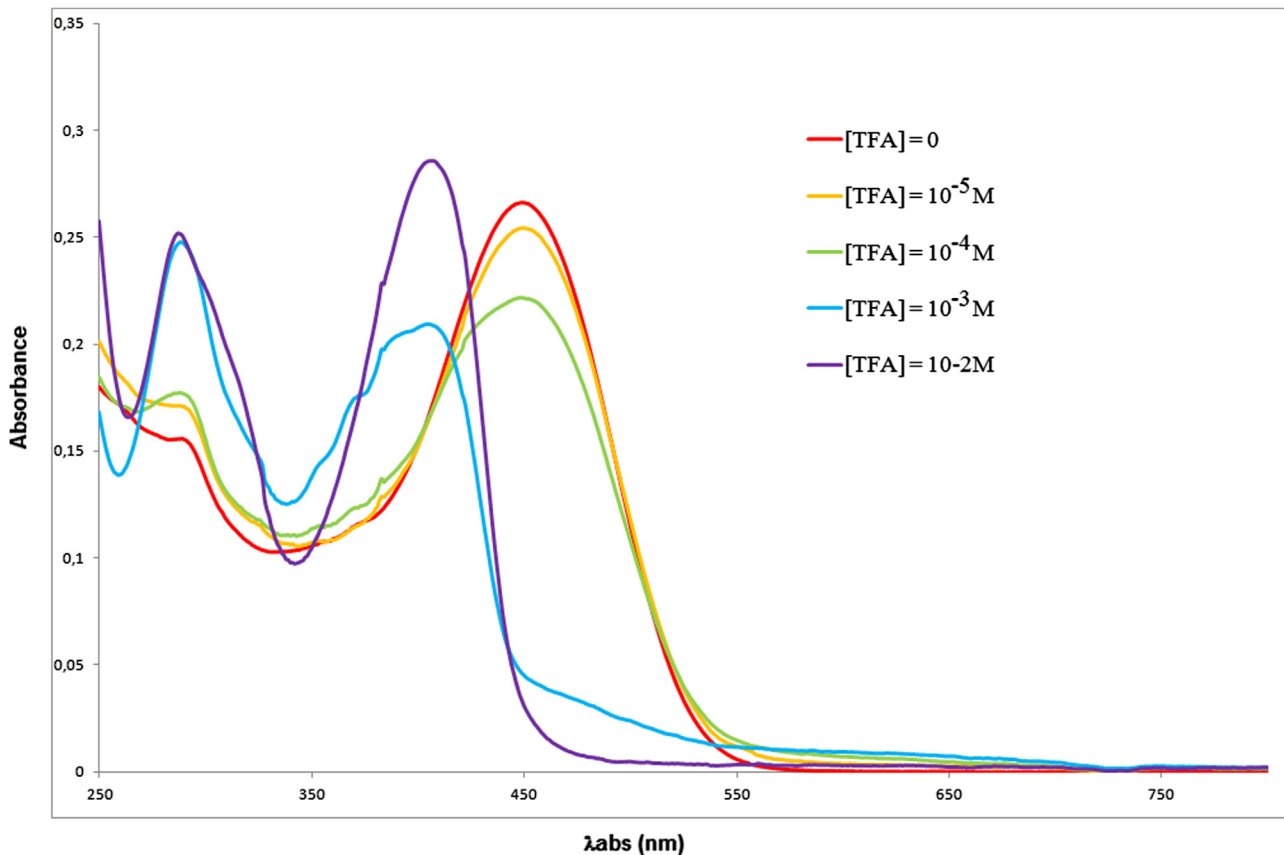


Fig. 3. UV/vis absorption change of **10** in CH_2Cl_2 ($c=1.1 \cdot 10^{-5} \text{ M}$) with increasing TFA concentration.

Table 3Electrochemical data^a for compounds **1**, **2**, **4**, **5**, **6**, **7**, **8**, **10**, and **12**

Compound	$E_{\text{ox}}(1)$ ^b	$E_{\text{ox}}(2)$ ^b	$E_{\text{ox}}(3)$	$E_{1/2 \text{ red}}$
1 ^c	0.20			-2.21
2 ^c	0.25			-2.06
4a	0.27	0.47 ^d		-1.98
4b	0.10	0.30 ^d		-1.92
4c	0.27			- ^e
5a	0.24	0.33 ^b	0.56	-1.94
5b	0.22	0.31 ^b	0.63	- ^e
6a	0.23			- ^e
6b	0.21	0.49 ^b	0.56	- ^e
7a	0.23	0.51 ^d		-1.90
7b	0.19	0.52 ^d		-2.00
8a	0.25	0.55 ^b		- ^e
8b	0.20	0.52 ^b		- ^e
10	0.26			-1.88
12	0.29			- ^e

^a Potentials were determined by cyclic voltammetry in $\text{CH}_2\text{Cl}_2-\text{Bu}_4\text{NBF}_4$ (0.1 M) with a Pt disk working electrode, $v=0.1 \text{ V s}^{-1}$, and are given versus the ferrocene/ferricinium couple.

^b Irreversible peak.

^c Data from Ref. 16.

^d Quasi-reversible system.

^e Undefined reduction peak.

natural atomic orbital (NAO) charge analysis. The charge of the diazino fragments are -0.16, -0.12, -0.12, -0.15, and -0.28 in **4a**, **6a**, **8a**, **4b**, and **5a**, respectively, whereas the charge of the $\text{C}_5\text{H}_4\text{OPh}_2$ unit is 0.22, 0.18, 0.17, 0.15, and 0.19, respectively. Thus, the amount of charge transfer from the diphenylpyran fragment to the diazino ring is comparable in the **4a**, **6a**, **8a**, and **4b** series, with a slightly stronger transfer in the case of **4a**. In the case of the symmetrical **5a** molecule, the transfer to the central heterocycle is larger, due to the presence of two $\text{C}_5\text{H}_4\text{OPh}_2$ donor units. The dipole moments (Table 4) reflect this fragment charge distribution, combined with the different charge distributions over the diazino fragments. Unsurprisingly, the MO diagrams of the five computed compounds are quite similar and only that of **4a** is shown in Fig. 6. Compounds **4a**, **4b**, **6a**, and **8a** exhibit a rather high-lying HOMO, which can be described as an antibonding combination of the highest π -bonding orbitals of the $(\text{CH})_n$ bridge and of the C_5O heterocycle. Their LUMO's are much more equally spread out over the whole molecule, whereas the LUMO+1 is localized on the diphenylpyran moiety. In the case of **5a**, all these orbitals are doubled.

The geometries of the monocationic and monoanionic forms of compounds **4a**, **4b**, **5a**, **6a**, and **8a** have been also fully optimized in

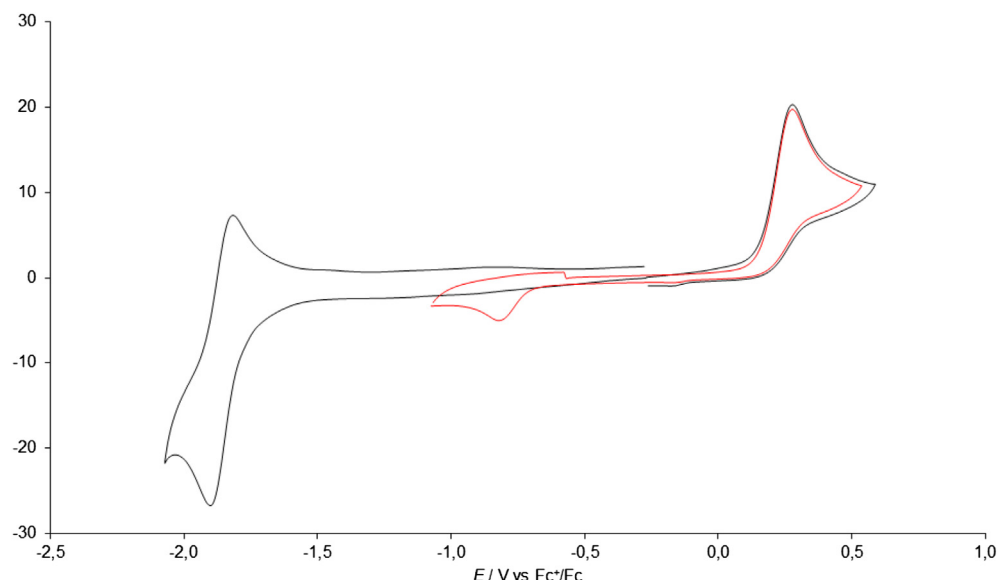


Fig. 4. Cyclic voltammograms of compound **10** at a Pt disk working electrode, in $\text{CH}_2\text{Cl}_2-\text{Bu}_4\text{NBF}_4$ (0.1 mol L⁻¹) at 298 K. Anodic and cathodic scan (black), anodic scan followed by a cathodic scan (red). All potentials are relative to the ferrocene/ferrocenium couple (Fc^+/Fc).

2.5. Computational studies

In order to shed some light on the electronic structure of the title compounds, DFT calculations have been performed on **4a**, **5a**, **6a**, **4b**, and **8a**. Their geometries were fully optimized with and without considering solvent effect corrections (see computational details) and little differences were found between the vacuum and solvent-corrected geometries, which are shown in Fig. 5. They exhibit a conjugated, near planar geometry, the phenyl substituents being slightly tilted by ~12–15° for obvious steric reasons. Relevant bond distances are given in Table 4. They indicate only little metrical differences along the conjugated backbone. The polyenic chains exhibit alternating longer (~1.42–1.47 Å) and shorter (~1.37–1.38 Å) bonds in accordance with BLA estimated by NMR, and the structure of the oxygen-containing heterocycle is clearly that of a methylenepyran. The small differences in the amount of conjugation along the molecules can also be evidenced from the

order to calculate their first ionization energy and their electron affinity (see Table 4). A reasonable linear correlation was found between the ionization energies computed with solvent corrections and the oxidation potentials recorded by cyclic voltammetry. A better agreement is even found if **5a** is removed from the fit. This is likely due to the fact that this symmetric molecule interacts differently with the electrolyte, which is not considered in the calculations. The corresponding correlations curves are illustrated in Fig. 7. They illustrate the similarities between **4a**, **6a**, and **8a**, and the slightly different behavior of **5a**.

In order to get a better insight into their optical properties, time-dependent DFT (TDDFT) calculations have been carried out on the five compounds (see computational details). The experimental absorption peaks of lowest energy, which are recorded at $\lambda_{\text{abs}}=444$, 440, 427, 469, and 503 nm for **4a**, **6a**, **8a**, **4b**, and **5a**, respectively (see Table 2) can be indexed to HOMO→LUMO transitions computed at 438, 428, 420, 477, and 483 nm, respectively. Thus, the associated

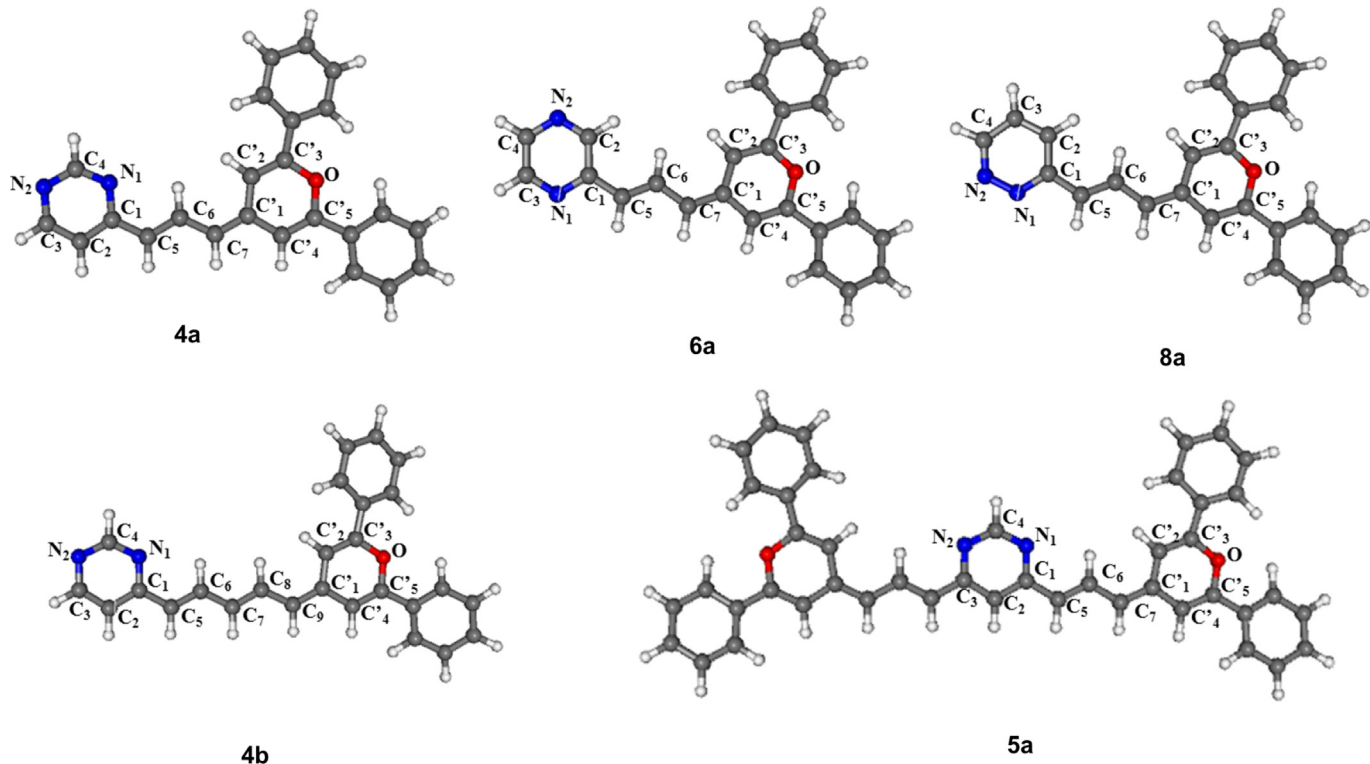


Fig. 5. The DFT-optimized molecular structures of **4a**, **6a**, and **8a** (top) and **4b** and **5a** (bottom).

Table 4

Relevant computed data for compounds **4a**, **5a**, **6a**, **4b**, and **8a** in dichloromethane (see [Computational details](#)). Interatomic distances are given in Å

	4a	6a	8a	5a	4b
HOMO–LUMO gap (eV)	3.02	3.04	3.10	2.72	2.86
Ionization energy (eV)	4.86	4.79	4.81	4.75	4.68
Electronic affinity (eV)	−2.71	−2.61	−2.58	−2.77	−2.81
C ₁ –C ₂	1.411	C ₁ –C ₂	1.418	C ₁ –C ₂	1.403
C ₂ –C ₃	1.387	C ₃ –C ₄	1.395	C ₂ –C ₃	1.403
N ₁ –C ₁	1.356	N ₁ –C ₁	1.350	N ₁ –C ₁	1.358
N ₁ –C ₄	1.328	N ₁ –C ₄	1.333	N ₁ –C ₄	1.331
N ₂ –C ₃	1.345	N ₂ –C ₂	1.327	N ₂ –C ₃	1.358
N ₂ –C ₄	1.338	N ₂ –C ₃	1.342	N ₁ –N ₂	N ₂ –C ₄
C ₁ –C ₅	1.447		1.452		1.450
C ₅ –C ₆	1.367		1.365		1.366
C ₆ –C ₇	1.423		1.427		1.425
C ₇ –C _{1'}		1.384	1.382	1.381	C ₇ –C ₈
C _{1'} –C _{2'}		1.445	1.447	1.447	C ₈ –C ₉
C _{2'} –C _{3'}		1.357	1.356	1.356	1.385
C _{3'} –O		1.369	1.369	1.369	1.445
C _{5'} –O		1.369	1.372	1.372	1.356
C _{5'} –C _{4'}		1.357	1.356	1.356	1.357
C _{1'} –C _{4'}		1.443	1.445	1.445	1.444
C _{3'} –C		1.470	1.470	1.470	1.470
C _{5'} –C		1.469	1.469	1.469	1.469
Dipole moment (Debye)	7.75	5.82	9.78	2.07	9.02

charge transfer is mainly from the molecule core to its ends. The two next absorption peaks at higher energy correspond to transitions from other occupied orbitals to the LUMO or LUMO+1. The emission wavelength involving the lowest excited singlet state (both HOMO and LUMO singly occupied) has also been calculated by TDDFT. The computed wavelengths are 569, 573, 560, 667, and 573 nm for **4a**, **6a**, **8a**, **4b**, and **5a**. These values are in a reasonable agreement with their

experimental λ_{abs} counterparts, which are 542, 550, 560, 535, and 600 nm, respectively (see [Table 2](#)).

Quadratic non-linear optical hyperpolarizabilities have been also computed for compounds **4a**, **6a**, **8a**, **4b**, and **5a** (see [Computational details](#)). The computed β_{static} values (in 10^{-30} esu) are 15, 13, 12, 31, and 17 in vacuum, respectively. When solvent (CH_2Cl_2) effect is considered they shift to 55, 43, 38, 119, and 54,

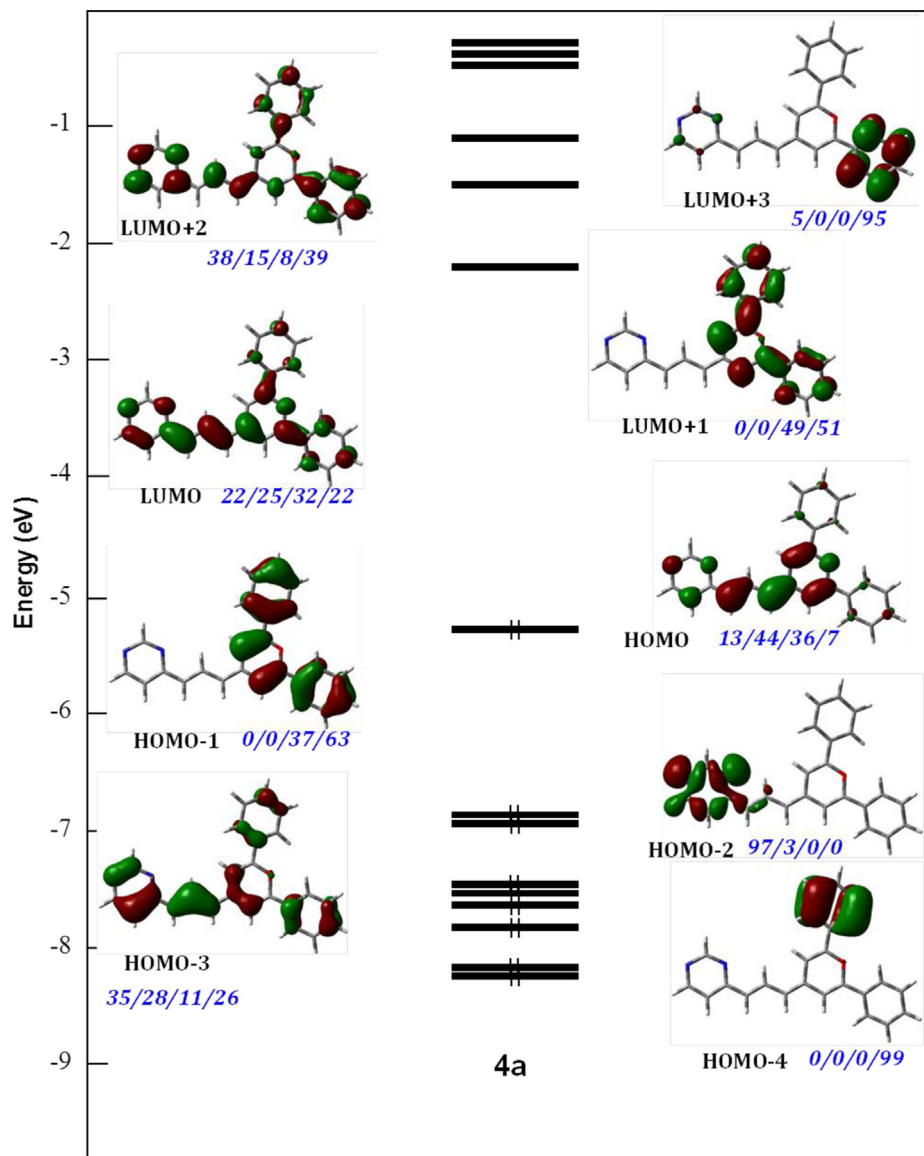


Fig. 6. MO diagram of compound 4a. The % localization of the MO's (in blue) corresponds to the following fragments: diazine/polyenic bridge/C₅H₂O ring/phenyl rings.

respectively. The corresponding β_{dynamic} values (in 10^{-30} esu) computed at 1907 nm in vacuum are 19, 17, 15, 41, and 22, respectively. When solvent effect is considered they shift to 79, 62, 54, 190, and 69, respectively. Although such computed results have probably to be taken only at a qualitative level, they are indicative of a strong molecular polarizability (especially **4b**) and suggest these compounds to have interesting second-order NLO properties. The β_{dynamic} values calculated in CH₂Cl₂ are in the same order than the experimental values obtained for amine substituted tetra(arylvinyl)bipyrimidine described in the literature ($\beta_0=110-130 \cdot 10^{-30}$ esu).²⁶

3. Conclusion

In conclusion, we have successfully synthesized and characterized a series of push–pull and V-shaped structures incorporating methylenepyran as pro-aromatic electron-donating moieties and diazine electron-attracting fragments. The optical properties of the dyes were studied: all compounds were colored and slightly fluorescent (except the pyridyl derivative **12**). These compounds exhibit intense halochromism properties, which depends of the π -conjugated core: on one hand, in case of phenylenevinylene

derivatives, the protonation occurs on the pyranylidene part leading to a strongly emissive pyrylium salts, which is blue shifted in absorption. On the other hand, in case of diethylene and triethylene derivatives, the protonation occurs on the diazine fragments leading to a red shifted absorption. Cyclic voltammetry and DFT calculation have shown that the donors and acceptor are engaged similarly in ICT in all the compounds. Quadratic non-linear optical hyperpolarizabilities of selected compounds have been also computed and suggest that these compounds are potential second-order NLO chromophores.

4. Experimental section

4.1. General methods

In air and moisture-sensitive reactions, all glassware was flame-dried and cooled under nitrogen. ¹BuOK was purified by the procedure described by Glinka²⁷ and kept under nitrogen, all other commercially available reactants are used without further purification. Compounds **3**,^{8c,8d,28} 2,6-diphenyl-4H-pyran-4-yl triphenylphosphonium tetrafluoroborate salt¹⁹ and 4-methyl-2,6-di-

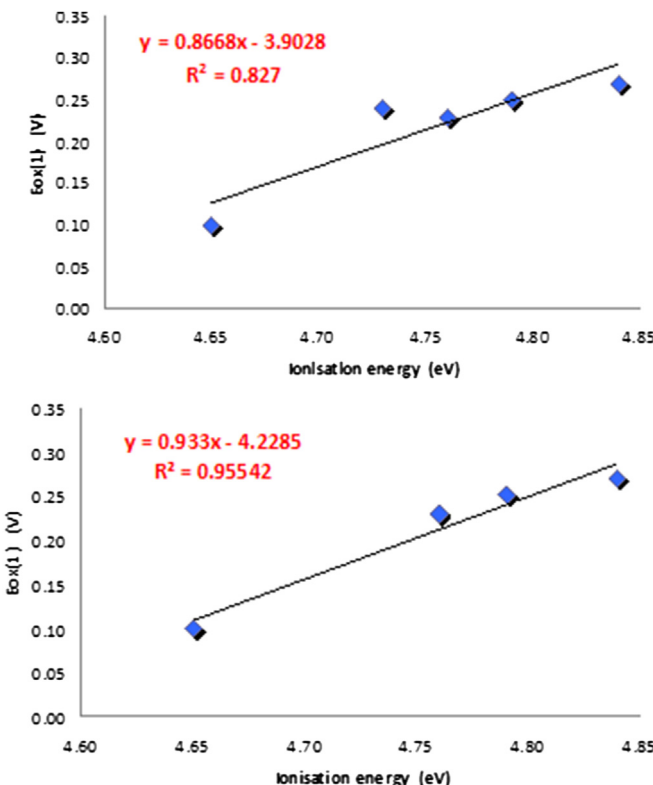


Fig. 7. Top: Linear correlation between the computed first ionization energy and E_{ox} of **4a**, **4b**, **5a**, **6a**, and **8a** (top) and **4a**, **4b**, **6a**, and **8a** (bottom). Solvent corrections were assumed in the calculations.

pyridin-2-yl-pyrimidine²¹ were prepared as previously described. NMR spectra were acquired at room temperature on a Bruker AC-300 spectrometer. Chemical shifts are given in parts per million relative to TMS (^1H , 0.0 ppm) and CDCl_3 (^{13}C , 77.0 ppm). Acidic impurities in CDCl_3 were removed by treatment with anhydrous K_2CO_3 . High resolution mass analyses were performed at the 'Centre Régional de Mesures Physiques de l'Ouest' (CRMPO, University of Rennes1) using a Bruker MicroTOF-Q II apparatus. UV/vis spectra were recorded with a UVIKON xm SECOMAM spectrometer using standard 1 cm quartz cells. Fluorescence spectra were recorded using Spex FluoroMax-3 Jobin-Yvon Horiba apparatus. Measurements were performed at room temperature with solutions of $\text{OD} < 0.1$ to avoid re-absorption of the emitted light, and data were corrected with a blank and from the variations of the detector with the emitted wavelength. Fluorescence quantum yield were measured according to Crosby comparative method²⁹ using quinine bisulfate in 1 M H_2SO_4 ($\Phi_F = 0.54$) or rhodamine in ethanol ($\Phi_F = 1.00$) as reference. Cyclic voltammetry experiments were performed on a μ -AUTOLAB III potentiostat monitored by a computer. All the potentials were standardized against the ferrocene–ferricinium couple. Ferrocene was added as an internal standard at the end of the experiments. A three-electrode cell was used, equipped with a platinum wire auxiliary electrode, a platinum working electrode and a silver wire as a quasi-reference electrode.

4.2. General procedure A for condensation reaction

Methyldiazine derivative (1 mmol) and compound **3** (1.1 equiv per methyl group) were dissolved in THF (20 mL). $^t\text{BuOK}$ (1.5 equiv per methyl group) was slowly added at room temperature. The solution, which immediately turned brown, was then refluxed

overnight. After cooling, water was added, THF was evaporated and the mixture extracted with CH_2Cl_2 , dried over MgSO_4 and the solvent removed under vacuum.

4.3. (*E*)-4-[3-(2,6-Diphenyl-pyran-4-ylidene)-propenyl]-pyrimidine (**4a**)

Red solid; obtained according to general procedure and purified by column chromatography (SiO_2 , Petroleum ether/EtAcO, 1:1); yield 44% (154 mg); mp: 201–202 °C; ^1H NMR (500 MHz, CDCl_3) δ 5.88 (d, 1H, $J = 12.5$ Hz), 6.37 (d, 1H, $J = 14.5$ Hz), 6.49 (d, 1H, $J = 1.0$ Hz), 7.01 (d, 1H, $J = 1$ Hz), 7.12 (d, 1H, $J = 5.5$ Hz), 7.51–7.45 (m, 6H), 7.81–7.79 (m, 2H), 7.89–7.87 (m, 2H), 8.11 (dd, 1H, $J_1 = 12.5$ Hz, $J_2 = 14.5$ Hz), 8.55 (d, 1H, $J = 5.5$ Hz), 9.08 (s, 1H); ^{13}C NMR and JMOD (125 MHz, CDCl_3) δ 163.0 (C), 158.7 (CH), 156.7 (CH), 153.6 (C), 153.0 (C), 135.8 (C), 133.2 (CH), 132.9 (C), 132.7 (C), 129.9 (CH), 129.7 (CH), 128.8 (CH), 125.2 (CH), 124.8 (CH), 123.6 (CH), 118.3 (CH), 113.7 (CH), 108.4 (CH), 102.5 (CH). HRMS (ESI/ASAP) m/z calculated for $\text{C}_{24}\text{H}_{19}\text{N}_2\text{O}$ [M+H]⁺ 351.1497, found 351.1493.

4.4. (*E,E*)-4-[5-(2,6-Diphenyl-pyran-4-ylidene)-penta-1,3-dienyl]-pyrimidine (**4b**)

Red solid; obtained according to general procedure and purified by column chromatography (SiO_2 , Petroleum ether/EtAcO, 1:1); yield 65% (244 mg); mp: 242–243 °C; ^1H NMR (500 MHz, CDCl_3) δ 5.78 (d, 1H, $J = 12.4$ Hz), 6.43–6.37 (m, 3H), 6.79 (s, 1H), 7.06 (dd, 1H, $J_1 = 14$ Hz, $J_2 = 13$ Hz), 7.14 (d, 1H, $J = 5.5$ Hz), 7.50–7.41 (m, 6H), 7.68 (dd, 1H, $J_1 = 12.4$ Hz, $J_2 = 14.7$ Hz), 7.76–7.75 (m, 2H), 7.82–7.80 (m, 2H), 8.55 (d, 1H, $J = 5.5$ Hz), 9.06 (s, 1H); ^{13}C NMR and JMOD (125 MHz, CDCl_3) δ 162.8 (C), 158.8 (CH), 156.8 (CH), 153.0 (C), 152.3 (C), 139.0 (CH), 135.1 (CH), 133.3 (C), 133.0 (C), 132.8 (C), 129.7 (CH), 129.5 (CH), 128.81 (CH), 128.76 (CH), 127.2 (CH), 125.6 (CH), 125.0 (CH), 124.7 (CH), 118.0 (CH), 114.7 (CH), 108.5 (CH), 102.3 (CH). HRMS (ESI/ASAP) m/z calculated for $\text{C}_{26}\text{H}_{21}\text{N}_2\text{O}$ [M+H]⁺ 377.1654, found 377.1654.

4.5. (*E*)-4-[3-(2,6-Di-tert-butyl-pyran-4-ylidene)-propenyl]-pyrimidine (**4c**)

Yellow solid; obtained according to general procedure and purified by column chromatography (SiO_2 , Petroleum ether/EtAcO, 7:3); yield 43% (133 mg); mp: 69–70 °C; ^1H NMR (500 MHz, CDCl_3) δ 1.19 (s, 9H), 1.24 (s, 9H), 5.58 (d, 1H, $J = 12.5$ Hz), 5.70 (d, 1H, $J = 1.5$ Hz), 6.20 (d, 1H, $J = 14.5$ Hz), 6.23 (d, 1H, $J = 1.5$ Hz), 7.04 (d, 1H, $J = 5.0$ Hz), 8.11 (dd, 1H, $J_1 = 12.5$ Hz, $J_2 = 14.5$ Hz), 8.46 (d, 1H, $J = 5.0$ Hz), 8.99 (s, 1H); ^{13}C NMR and JMOD (125 MHz, CDCl_3) δ 165.1 (C), 164.5 (C), 163.4 (C), 158.6 (CH), 156.3 (CH), 137.4 (C), 133.8 (CH), 121.6 (CH), 117.8 (CH), 110.8 (CH), 105.0 (CH), 98.9 (CH), 35.6 (C), 35.5 (C), 27.9 (CH), 27.8 (CH). HRMS (ESI/ASAP) m/z calculated for $\text{C}_{20}\text{H}_{27}\text{N}_2\text{O}$ [M+H]⁺ 311.2123, found 311.2122.

4.6. (*E,E*)-4,6-Bis-[3-(2,6-diphenyl-pyran-4-ylidene)-propenyl]-pyrimidine (**5a**)

Red solid; obtained according to general procedure and purified by column chromatography (SiO_2 , Petroleum ether/EtAcO, 1:1); yield 64% (397 mg); mp: >250 °C; ^1H NMR (500 MHz, CDCl_3) δ 5.86 (d, 2H, $J = 12$ Hz), 6.35 (d, 2H, $J = 14.5$ Hz), 6.45 (d, 2H, $J = 1.0$ Hz), 6.88 (s, 1H), 7.01 (d, 2H, $J = 1$ Hz), 7.50–7.41 (m, 12H), 7.77–7.75 (m, 4H), 7.86–7.84 (m, 4H), 8.06 (dd, 2H, $J_1 = 12$ Hz, $J_2 = 14.5$ Hz), 8.95 (s, 1H); ^{13}C NMR and JMOD (125 MHz, CDCl_3) δ 162.8 (C), 153.3 (C), 152.7 (C), 135.2 (C), 133.0 (C), 132.8 (C), 132.2 (CH), 129.8 (CH), 129.6 (CH), 128.8 (CH), 125.2 (CH), 124.8 (CH), 124.5 (CH), 116.2 (CH), 114.1 (CH), 108.5 (CH), 102.6 (CH). HRMS (ESI/ASAP) m/z calculated for $\text{C}_{44}\text{H}_{33}\text{N}_2\text{O}_2$ [M+H]⁺ 621.2542, found 621.2539.

4.7. (*E,E*)4,6-Bis-[3-(2,6-*tert*-butyl-pyran-4-ylidene)-propenyl]-pyrimidine (5b)

Red solid; obtained according to general procedure and purified by column chromatography (SiO_2 , Petroleum ether/EtAcO, 1:1); yield 73% (394 mg); mp: 124–125 °C; ^1H NMR (300 MHz, CDCl_3) δ 1.21 (s, 9H), 1.25 (s, 9H), 5.59 (d, 2H, $J=12.3$ Hz), 5.69 (d, 2H, $J=1$ Hz), 6.19 (d, 2H, $J=14.7$ Hz), 6.24 (d, 2H, $J=1$ Hz), 6.80 (s, 1H), 7.89 (dd, 2H, $J_1=12.3$ Hz, $J_2=14.5$ Hz), 8.87 (s, 1H); ^{13}C NMR and JMOD (125 MHz, CDCl_3) δ 164.6 (C), 163.9 (C), 162.9 (C), 158.2 (CH), 136.4 (C), 132.5 (CH), 122.6 (CH), 115.1 (CH), 111.2 (CH), 104.9 (CH), 99.0 (CH), 35.8 (C), 35.4 (C), 27.9 (CH₃), 27.8 (CH₃), HRMS (ESI/ASAP) m/z calculated for $\text{C}_{36}\text{H}_{49}\text{N}_2\text{O}$ [M+H]⁺ 541.3794, found 541.3782.

4.8. (*E*)2-[3-(2,6-Diphenyl-pyran-4-ylidene)-propenyl]-pyrazine (6a)

Red solid; obtained according to general procedure and purified by crystallization from $\text{CH}_2\text{Cl}_2/n$ -heptane; yield 47% (163 mg); mp: 161–162 °C; ^1H NMR (300 MHz, CDCl_3) δ 5.87 (d, 1H, $J=11.7$ Hz), 6.44 (d, 1H, $J=1.0$ Hz), 6.46 (d, 1H, $J=14.4$ Hz), 6.95 (d, 1H, $J=1$ Hz), 7.51–7.41 (m, 6H), 7.78–7.75 (m, 2H), 7.86–7.83 (m, 2H), 7.91 (dd, 1H, $J_1=11.7$ Hz, $J_2=14.4$ Hz), 8.26 (d, 1H, $J=2.4$ Hz), 8.46 (s, 2H); ^{13}C NMR and JMOD (125 MHz, CDCl_3) δ 153.0 (C), 152.5 (C), 152.3 (C), 144.2 (CH), 143.7 (CH), 141.0 (CH), 134.0 (C), 133.0 (C), 132.8 (C), 130.8 (CH), 129.6 (CH), 129.4 (CH), 128.7 (CH), 125.1 (CH), 124.7 (CH), 122.4 (CH), 114.2 (CH), 108.3 (CH), 102.4 (CH). HRMS (ESI/ASAP) m/z calculated for $\text{C}_{24}\text{H}_{19}\text{N}_2\text{O}$ [M+H]⁺ 351.1497, found 351.1498.

4.9. (*E*)2-[3-(2,6-Di-*tert*-butyl-pyran-4-ylidene)-propenyl]-pyrazine (6b)

Yellow sticky solid; obtained according to general procedure and purified by column chromatography (SiO_2 , Petroleum ether/EtAcO, 1:1); yield 65% (201 mg); ^1H NMR (300 MHz, CDCl_3) δ 1.19 (s, 9H), 1.24 (s, 9H), 5.59 (d, 1H, $J=12$ Hz), 5.66 (d, 1H, $J=1.8$ Hz), 6.18 (d, 1H, $J=1.8$ Hz), 6.33 (d, 1H, $J=15$ Hz), 7.76 (dd, 1H, $J_1=12$ Hz, $J_2=15$ Hz), 8.20 (d, 1H, $J=2.4$ Hz), 8.41–8.40 (m, 2H); ^{13}C NMR and JMOD (125 MHz, CDCl_3) δ 164.4 (C), 163.7 (C), 159.9 (C), 144.0 (CH), 143.4 (CH), 140.4 (CH), 135.4 (C), 131.3 (CH), 120.5 (CH), 111.2 (CH), 104.7 (CH), 98.7 (CH), 35.7 (C), 35.3 (C), 27.9 (CH), 27.8 (CH). HRMS (ESI/ASAP) m/z calculated for $\text{C}_{20}\text{H}_{27}\text{N}_2\text{O}$ [M+H]⁺ 311.2123, found 311.2125.

4.10. (*E*)2-[3-(2,6-Diphenyl-pyran-4-ylidene)-propenyl]-quinoxaline (7a)

Red solid; obtained according to general procedure and purified by column chromatography (SiO_2 , Petroleum ether/EtAcO, 1:1); yield 51% (204 mg); mp: 210–211 °C; ^1H NMR (300 MHz, CDCl_3) δ 5.93 (d, 1H, $J=12.3$ Hz), 6.48 (s, 1H), 6.65 (d, 1H, $J=15$ Hz), 7.02 (d, 1H, $J=1$ Hz), 7.51–7.41 (m, 6H), 7.59–7.65 (m, 1H), 7.68–7.74 (m, 1H), 7.76–7.79 (m, 2H), 7.85–7.88 (m, 2H), 8.02–8.04 (m, 2H), 8.06 (dd, 1H, $J_1=12.3$ Hz, $J_2=15$ Hz), 8.83 (s, 1H); ^{13}C NMR and JMOD (125 MHz, CDCl_3) δ 153.3 (C), 152.6 (C), 151.7 (C), 145.4 (CH), 142.9 (C), 140.9 (C), 134.8 (C), 133.0 (C), 132.7 (C), 130.0 (CH), 129.8 (CH), 129.5 (CH), 129.0 (CH), 128.7 (CH), 128.1 (CH), 125.1 (CH), 124.7 (CH), 123.4 (CH), 114.5 (CH), 108.5 (CH), 102.5 (CH). HRMS (ESI/ASAP) m/z calculated for $\text{C}_{28}\text{H}_{21}\text{N}_2\text{O}$ [M+H]⁺ 401.1654, found 401.1655.

4.11. (*E*)2-[3-(2,6-Di-*tert*-butyl-pyran-4-ylidene)-propenyl]-quinoxaline (7b)

Red solid; obtained according to general procedure and purified by column chromatography (SiO_2 , Petroleum Ether/EtAcO, 7:3);

yield 68% (243 mg); mp: 69–70 °C; ^1H NMR (300 MHz, CDCl_3) δ 1.13 (s, 9H), 1.19 (s, 9H), 5.60 (d, 1H, $J=12$ Hz), 5.65 (d, 1H, $J=2$ Hz), 6.20 (d, 1H, $J=2$ Hz), 7.02 (d, 1H, $J=15$ Hz), 7.48–7.53 (m, 1H), 7.57–7.63 (m, 1H), 7.80–7.81 (m, 3H), 8.74 (s, 1H); ^{13}C NMR and JMOD (125 MHz, CDCl_3) δ 164.8 (C), 164.2 (C), 152.2 (C), 145.3 (CH), 142.9 (C), 140.7 (C), 136.4 (C), 132.9 (CH), 129.9 (CH), 129.0 (CH), 128.6 (CH), 127.8 (CH), 121.5 (CH), 111.5 (CH), 105.0 (CH), 98.9 (CH), 35.8 (C), 35.4 (C), 27.9 (CH₃), 27.8 (CH₃). HRMS (ESI/ASAP) m/z calculated for $\text{C}_{24}\text{H}_{29}\text{N}_2\text{O}$ [M+H]⁺ 361.2280, found 361.2280.

4.12. (*E*)3-[3-(2,6-Diphenyl-pyran-4-ylidene)-propenyl]-pyridazine (8a)

Red solid; obtained according to general procedure and purified by column chromatography (SiO_2 , Petroleum ether/EtAcO, 1:1); yield 43% (145 mg); mp: 160–161 °C; ^1H NMR (300 MHz, CDCl_3) δ 5.89 (d, 1H, $J=12$ Hz), 6.47 (d, 1H, $J=1.0$ Hz), 6.55 (d, 1H, $J=15$ Hz), 6.99 (d, 1H, $J=1$ Hz), 7.39–7.35 (m, 2H), 7.51–7.43 (m, 6H), 7.80–7.78 (m, 2H), 7.88–7.86 (m, 2H), 7.05 (dd, 1H, $J_1=12$ Hz, $J_2=15$ Hz), 8.94 (dd, 1H, $J_1=1.5$ Hz, $J_2=4.5$ Hz); ^{13}C NMR and JMOD (125 MHz, CDCl_3) δ 157.5 (C), 151.6 (C), 150.8 (C), 146.8 (CH), 132.6 (C), 131.5 (C), 131.3 (C), 129.4 (CH), 128.1 (CH), 127.9 (CH), 127.2 (CH), 124.6 (CH), 123.5 (CH), 123.2 (CH), 122.7 (CH), 121.4 (CH), 112.4 (CH), 106.7 (CH), 100.8 (CH). HRMS (ESI/ASAP) m/z calculated for $\text{C}_{24}\text{H}_{19}\text{N}_2\text{O}$ [M+H]⁺ 351.1497, found 351.1496.

4.13. (*E*)3-[3-(2,6-Di-*tert*-butyl-pyran-4-ylidene)-propenyl]-pyridazine (8b)

Yellow solid; obtained according to general procedure and purified by column chromatography (SiO_2 , Petroleum ether/EtAcO, 1:1); yield 59% (182 mg); mp: 141–142 °C; ^1H NMR (400 MHz, CDCl_3) δ 1.16 (s, 9H), 1.20 (s, 9H), 5.57 (d, 1H, $J=12$ Hz), 5.64 (d, 1H, $J=1.0$ Hz), 6.15 (d, 1H, $J=1$ Hz), 6.37 (d, 1H, $J=15$ Hz), 7.33–7.23 (m, 2H), 7.81 (dd, 1H, $J_1=12$ Hz, $J_2=15$ Hz), 8.94 (dd, 1H, $J_1=1.2$ Hz, $J_2=4.5$ Hz); ^{13}C NMR and JMOD (125 MHz, CDCl_3) δ 164.4 (C), 163.7 (C), 159.3 (C), 148.0 (CH), 135.9 (C), 131.3 (CH), 126.0 (CH), 123.8 (CH), 121.0 (CH), 111.0 (CH), 104.6 (CH), 98.6 (CH), 35.7 (C), 35.3 (CH), 27.9 (CH₃), 27.7 (CH₃). HRMS (ESI/ASAP) m/z calculated for $\text{C}_{20}\text{H}_{27}\text{N}_2\text{O}$ [M+H]⁺ 311.2123, found 311.2124.

4.14. General procedure for the synthesis of aldehydes 9 and 11

A mixture of methyldiazine (4 mmol) and benzene-1,4-dicarboxaldehyde mono-(diethyl acetal) (832 mg, 4 mmol) in an aqueous solution (30 mL) of sodium hydroxide (5 M) containing Aliquat 336 (0.1 mol) was heated under reflux for 15 h. After cooling, the solid was filtered off, washed with water and dried. The solid was then dissolved in acetone (50 mL), and a small amount (0.5 mL) of concentrated hydrochloric acid was added under agitation. The precipitate formed was filtered off and dissolved in diluted ammonia aqueous solution. The reaction mixture was extracted with dichloromethane (3×50 mL), the combined organic layer were washed with water, dried over MgSO_4 , and the solvent was removed by evaporation under reduced pressure. A solid is obtained and used without further purification.

4.15. 4-(2-Quinolin-2-yl-vinyl)-benzaldehyde (9)

Beige solid; yield 86% (894 mg); mp: 177–178 °C; ^1H NMR (500 MHz, CDCl_3) δ 7.53 (d, 1H, $J=16.5$ Hz), 7.79–7.73 (m, 2H), 7.81 (d, 2H, $J=8.0$ Hz), 7.93 (d, 1H, $J=16.5$ Hz), 7.94 (d, 2H, $J=8.0$ Hz), 8.10–8.08 (m, 2H), 9.05 (s, 1H), 10.04 (s, 1H); ^{13}C NMR and JMOD (125 MHz, CDCl_3) δ 191.5 (CH), 149.8 (C), 144.6 (CH), 142.5 (C), 141.91

(C), 141.85 (C), 136.4 (C), 134.8 (CH), 130.6 (CH), 130.3 (CH), 129.8 (CH), 129.4 (CH), 129.3 (CH), 128.4 (CH), 127.7 (CH).

4.16. General procedure for the synthesis of compounds 10 and 12

Small excess of *n*-butyllithium 2.5 M in hexanes (0.88 mL, 2.2 mmol) was added dropwise at –78 °C, under a nitrogen atmosphere, to a degassed solution of 2,6-diphenyl-4*H*-pyran-4-yl triphenylphosphonium tetrafluoroborate salt (1.16 g, 2.0 mmol) in dry THF (20 mL). After 15 min, aldehyde **9** or **11** (1.8 mmol) was added. The solution was stirred at –78 °C for 30 min, and allowed to warm to room temperature for 2 h. THF was evaporated and the residue dissolved in a mixture of CH₂Cl₂ and water 1:1 (100 mL) and the organic layer separated. The aqueous layer was extracted with CH₂Cl₂ (2×50 mL). The combined organic extracts were dried with MgSO₄ and the solvents evaporated.

4.17. 2-[2-{4-(2,6-Diphenyl-pyran-4-ylidenemethyl)-phenyl}-vinyl]-quinoxaline (10)

The crude product was purified by column chromatography (SiO₂, Petroleum ether/EtAcO, 7:3) followed by crystallization from CH₂Cl₂/*n*-heptane; orange solid; yield 52% (446 mg); mp: 199–200 °C; ¹H NMR (500 MHz, CDCl₃) δ 5.96 (s, 1H), 6.46 (s, 1H), 7.07 (s, 1H), 7.38 (d, 1H, *J*=16 Hz), 7.41–7.49 (m, 8H), 7.66 (d, 2H, *J*=8 Hz), 7.71–7.69 (m, 1H), 7.76–7.74 (m, 1H), 7.80–7.77 (m, 4H), 7.88 (d, 1H, *J*=16 Hz), 8.07 (d, 2H, *J*=8 Hz), 9.10 (s, 1H); ¹³C NMR and JMOD (125 MHz, CDCl₃) δ 153.2 (C), 151.2 (C), 151.0 (C), 144.6 (CH), 142.6 (C), 141.5 (C), 140.0 (C), 136.3 (CH), 133.4 (C), 133.2 (C), 133.1 (C), 130.4 (C), 130.3 (CH), 129.5 (CH), 129.2 (CH), 129.1 (CH), 128.72 (CH), 128.69 (CH), 128.1 (CH), 127.8 (CH), 125.0 (CH), 124.6 (CH), 124.2 (CH), 113.8 (CH), 108.8 (CH), 102.2 (CH). HRMS (ESI) *m/z* calculated for C₃₄H₂₅N₂O [M+H]⁺ 477.1966, found 477.1964.

4.18. (E) 4-[2-(2,6-Di-pyridin-2-yl-pyrimidin-4-yl)-vinyl]-benzaldehyde (11)

Beige solid obtained according to general procedure; yield 94% (342 mg); mp: 94–95 °C; ¹H NMR (500 MHz, CDCl₃) δ 7.47–7.45 (m, 2H), 7.53 (d, 1H, *J*=16.5 Hz), 7.81 (d, 2H, *J*=8.0 Hz), 7.93–7.91 (m, 2H), 7.93 (d, 2H, *J*=8.0 Hz), 8.08 (d, 1H, *J*=16.5 Hz), 8.56 (s, 1H), 8.72–8.70 (m, 1H), 8.75–8.73 (m, 1H), 8.79–8.78 (m, 1H), 8.92–8.91 (m, 1H), 10.04 (s, 1H); ¹³C NMR and JMOD (125 MHz, CDCl₃) δ 191.6 (CH), 164.04 (C), 164.02 (C), 632.7 (C), 155.2 (C), 154.0 (C), 150.2 (CH), 149.5 (CH), 141.8 (C), 137.2 (CH), 137.0 (CH), 136.5 (C), 135.9 (CH), 130.3 (CH), 130.1 (CH), 128.1 (CH), 125.6 (CH), 124.9 (CH), 124.1 (CH), 122.2 (CH), 113.5 (CH).

4.19. (E)4-[2-{4-(2,6-Diphenyl-pyran-4-ylidenemethyl)-phenyl}-vinyl]-2,6-di-pyridin-2-yl-pyrimidine (12)

Crude product purified by crystallization from CHCl₃/*n*-heptane; Dark red solid; yield 60% (348 mg); mp: 208 °C (dec); ¹H NMR (500 MHz, THF-*d*₈) δ 6.02 (s, 1H), 6.44 (d, 1H, *J*=2 Hz), 7.17 (d, 1H, *J*=2 Hz), 7.51–7.39 (m, 10H), 7.74 (d, 2H, *J*=8 Hz), 7.87–7.85 (m, 4H), 7.97–7.90 (m, 3H), 8.22 (d, 1H, *J*=16 Hz), 8.50 (s, 1H), 8.67–8.65 (m, 1H), 8.76–8.74 (m, 1H), 8.78–8.77 (m, 1H), 8.83–8.82 (m, 1H); ¹³C NMR and JMOD (125 MHz, THF-*d*₈) δ 165.5 (C), 164.4 (C), 156.6 (C), 155.2 (C), 154.0 (C), 151.8 (C), 150.6 (CH), 150.5 (CH), 141.0 (C), 138.0 (CH), 137.9 (CH), 137.2 (CH), 134.4 (C), 134.3 (C), 134.2 (C), 131.1 (C), 130.2 (CH), 129.9 (CH), 129.5 (CH), 129.4 (CH), 129.0 (CH), 128.9 (CH), 126.31 (CH), 126.29 (CH), 125.8 (CH), 125.4 (CH), 125.3 (CH), 124.3 (CH), 122.6 (CH), 115.1 (CH), 114.0 (CH), 110.0 (CH), 103.0 (CH). HRMS (ESI) *m/z* calculated for C₄₀H₂₈N₄ONa [M+Na]⁺ 603.2161, found 603.2163.

5. Computational details

Geometry optimizations were carried out using the Gaussian 09 package,³⁰ employing the PBE0 functional,³¹ and using the standard double-ξ LANL2DZ basis set³² augmented with Ahlrichs polarization functions.³³ All stationary points were fully characterized via analytical frequency calculations as true minima (no imaginary values). Solvent (CH₂Cl₂) effects have been taken into account using the PCM model.³⁴ The geometries obtained from DFT calculations were used to perform natural atomic orbital analysis with the NBO 5.0 program.³⁵ The composition of the molecular orbitals was calculated using the AOMix program.³⁶ The ionization energies and electron affinities discussed above have been calculated considering the energies of the optimized neutral and ionic structures (solvent corrections performed). The UV visible transitions were calculated by means of TDDFT calculations³⁷ at the same level of theory. Only singlet-singlet transitions have been taken into account. Only the transitions with non-negligible oscillator strengths are discussed in the paper. Static and frequency-dependent electronic (hyper)polarizability tensor components β_{ijj} (*i,j*=x, y, z) were obtained through the Coupled-Perturbed Kohn–Sham procedure³⁸ using the more appropriate wb97XD functional³⁹ with the same basis set as above. Dynamic (hyper)polarizabilities are computed at the TDDFT level assuming a laser wavelength of 1907 nm ($\hbar\omega=0.023896$ a.u.) for the SHG [$\beta(-2\omega; \omega, \omega)$] NLO processes.

Acknowledgements

J.Y.S. thanks the Institut Universitaire de France for support.

Supplementary data

Supplementary data related to this article can be found at <http://dx.doi.org/10.1016/j.tet.2014.02.071>.

References and notes

- (a) Forrest, S. R.; Thompson, M. E. *Chem. Rev.* **2007**, *107*, 923; (b) Sullivan, P. A.; Dalton, L. R. *Acc. Chem. Res.* **2010**, *43*, 10; (c) Davies, J. A.; Elangovan, A.; Sullivan, P. A.; Olbricht, B. C. D. H.; Ewy, T. R.; Isborn, C. M.; Eichinger, B. E.; Robinson, B. H.; Reid, P. J.; Li, X.; Dalton, L. R. *J. Am. Chem. Soc.* **2008**, *130*, 10565.
- See for example: (a) Nepraš, M.; Almonasy, N.; Bureš, F.; Kulhánek, J.; Dvořák, M.; Michl, M. *Dyes Pigm.* **2011**, *91*, 466; (b) Achelle, S.; Barsella, A.; Baudequin, C.; Caro, B.; Robin-Le Guen, F. *J. Org. Chem.* **2012**, *77*, 4087; (c) Li, Y.; Ren, T.; Dong, W.-J. *J. Photochem. Photobiol. A* **2013**, *251*, 1.
- (a) Kraft, A.; Grimsdale, A. C.; Holmes, A. B. *Angew. Chem., Int. Ed.* **1998**, *37*, 402; (b) Mitzshe, U.; Bäuerle, P. *J. Mater. Chem.* **2000**, *10*, 1471; (c) Lo, S.-C.; Burn, P. L. *Chem. Rev.* **2007**, *107*, 1097.
- (a) Lin, Y.; Li, Y.; Zhan, X. *Chem. Soc. Rev.* **2012**, *41*, 4245; (b) Hagfeldt, A.; Boschloo, G.; Sun, L.; Kloot, L.; Pettersson, H. *Chem. Rev.* **2010**, *110*, 6595; (c) Günes, S.; Neugebauer, H.; Sariciftci, N. S. *Chem. Rev.* **2007**, *107*, 1324.
- (a) Zhang, C. Z.; Lu, C. G.; Zhu, J.; Lu, G. Y.; Wang, X.; Shi, Z. W.; Liu, F.; Cui, Y. P. *Chem. Mater.* **2006**, *18*, 6091; (b) Luo, J. D.; Hua, J. L.; Qin, J. G.; Cheng, J. Q.; Shen, Y. C.; Lu, Z. H.; Wang, P.; Ye, C. *Chem. Commun.* **2001**, *171*; (c) Verbiest, T.; Houbrechts, S.; Kauranen, M.; Clays, K.; Persoons, A. *J. Mater. Chem.* **1997**, *7*, 2175; (d) Wang, C.; Zhang, T.; Lin, W. *Chem. Rev.* **2012**, *112*, 1084; (e) Kim, H. M.; Cho, B. R. *Chem. Commun.* **2009**, 153.
- (a) Dalton, L. R. *J. Phys. Condens. Mater.* **2003**, *15*, R897; (b) Kuzyk, M. G. *J. Mater. Chem.* **2009**, *19*, 7444; (c) May, J. C.; Biaggio, I.; Bureš, F.; Diederich, F. *Appl. Phys. Lett.* **2007**, *90*, 1006.
- Tiemann, B. G.; Cheng, L.-T.; Marder, S.-R. *J. Chem. Soc., Chem. Commun.* **1993**, 735.
- (a) Faux, N.; Caro, B.; Robin-le Guen, F.; le Poul, P.; Nakatani, K.; Ishow, E. *J. Organomet. Chem.* **2005**, *690*, 4982; (b) Faux, N.; Robin-le Guen, F.; le Poul, P.; Caro, B.; Nakatani, K.; Ishow, E.; Golhen, S. *Eur. J. Inorg. Chem.* **2006**, 3489; (c) Millan, I.; Fuentealba, M.; Manzur, C.; Carrillo, D.; Faux, N.; Caro, B.; Robin-le Guen, F.; Sinbandhit, S.; Ledoux-Rak, I.; Hamon, J. R. *Eur. J. Inorg. Chem.* **2006**, 1131; (d) Andreu, R.; Carrasquer, L.; Franco, S.; Garín, J.; Orduna, J.; Martínez de Baroja, N.; Alicante, R.; Villacampa, B.; Allain, M. *J. Org. Chem.* **2009**, *74*, 6647; (e) Andreu, R.; Galán, E.; Garín, J.; Herrero, V.; Lacarra, E.; Orduna, J.; Alicante, R.; Villacampa, B. *J. Org. Chem.* **2010**, *75*, 1684; (f) Andreu, R.; Galán, E.; Orduna, J.; Villacampa, B.; Alicante, R.; López Navarrete, J. T.; Casado, J.; Garín, J. *Chem.—Eur. J.* **2011**, *17*, 826; (g) Galán, E.; Andreu, R.; Garín, J.; Orduna, J.; Villacampa, B.; Diósido, B. *Org. Biomol. Chem.* **2012**, *10*, 8684; (h) Porotnik, Y. M.; Hugues, V.; Blanchard-Desce, M.; Gryko, D. T. *Chem.—Eur. J.* **2012**, *18*, 9258; (i) Gauthier,

- S.; Vologdin, N.; Achelle, S.; Barsella, A.; Caro, B.; Robin-le Guen, F. *Tetrahedron* **2013**, *69*, 8392.
9. (a) Faux, N.; Robin-Le Guen, F.; le Poul, P.; Caro, B.; le Poul, N.; le Mest, Y.; Green, S. J.; le Roux, S.; Kahlal, S.; Saillard, J. Y. *Tetrahedron* **2007**, *63*, 7142; (b) Ba, F.; Cabon, N.; Robin-Le Guen, F.; le Poul, P.; le Poul, N.; le Mest, Y.; Golhen, S.; Caro, B. *Organometallics* **2008**, *27*, 6396.
 10. (a) Achelle, S.; Plé, N.; Turck, A. *RSC Adv.* **2011**, *1*, 364; (b) Achelle, S.; Plé, N. *Curr. Org. Synth.* **2012**, *9*, 163; (c) Achelle, S.; Baudequin, C.; Plé, N. *Dyes Pigm.* **2013**, *98*, 575; (d) Achelle, S.; Baudequin, C. *Targets Heterocycl. Syst.* **2013**, *17*, in press.
 11. (a) Liu, Z.; Shao, P.; Huang, Z.; Liu, B.; Chen, T.; Qin, J. *Chem. Commun.* **2008**, 2260; (b) Li, L.; Tian, Y. P.; Yang, J. X.; Sun, P. P.; Wu, J. Y.; Zhou, H. P.; Zhang, S. Y.; Jin, B. K.; Xing, X. J.; Wang, C. K.; Li, M.; Cheng, G. H.; Tang, H. H.; Huang, W. H.; Tao, X. T.; Jiang, M. H. *Chem.—Asian J.* **2009**, *4*, 668; (c) Liu, Z.; Chen, T.; Liu, B.; Huang, Z.-L.; Huang, T.; Li, S.; Xu, Y.; Qin, J. *J. Mater. Chem.* **2007**, *17*, 4685; (d) Liu, B.; Hu, X.-L.; Liu, J.; Zhao, Y.-D.; Huang, Z.-L. *Tetrahedron Lett.* **2007**, *48*, 5958; (e) Liu, B.; Zhang, H.-L.; Liu, J.; Zhao, Y.-D.; Luo, Q.-M.; Huang, Z.-L. *J. Mater. Chem.* **2007**, *17*, 2921; (f) Chen, D.; Zhong, C.; Dong, X.; Liu, Z.; Qin, J. *J. Mater. Chem.* **2012**, *22*, 4343; (g) Li, L.; Ge, J.; Wu, H.; Xu, Q.-H.; Yao, S. Q. *J. Am. Chem. Soc.* **2012**, *134*, 12157.
 12. (a) Boländer, A.; Kieser, D.; Voss, C.; Bauer, S.; Schön, C.; Burgold, S.; Bittner, T.; Hölzer, J.; Heyny-von Haußen, R.; Mall, G.; Goetschy, V.; Czech, C.; Knust, H.; Berger, R.; Herms, J.; Hilger, I.; Schmidt, B. *J. Med. Chem.* **2012**, *55*, 9170; (b) Vurth, L.; Hadad, C.; Achelle, S.; García-Martínez, J. C.; Rodríguez-López, J.; Stephan, O. *Colloid Polym. Sci.* **2012**, *290*, 1353; (c) Aranda, A. I.; Achelle, S.; Hammerer, F.; Mahuteau-Betzer, F.; Teulade-Fichou, M.-P. *Dyes Pigm.* **2012**, *95*, 400; (d) Hadad, C.; Achelle, S.; López-Solera, I.; García-Martínez, J. C.; Rodriguez-López, J. *Dyes Pigm.* **2013**, *97*, 230.
 13. (a) Shirai, K.; Yanagisawa, A.; Takahashi, H.; Fukunishi, K.; Matsuoka, M. *Dyes Pigm.* **1998**, *39*, 49; (b) Jaung, J. Y.; Matsuoka, M.; Fukunishi, K. *Dyes Pigm.* **1997**, *34*, 255; (c) Bureš, F.; Čermáková, H.; Kulhánek, J.; Ludwig, M.; Kuzník, W.; Kityk, I. V.; Mikyšek, T.; Růžička, A. *Eur. J. Org. Chem.* **2012**, 529.
 14. (a) Thomas, K.; Lin, J.; Tao, Y. *Chem. Mater.* **2002**, *14*, 2796; (b) Chang, D. W.; Ko, S.-J.; Kim, J. Y.; Dai, L.; Baek, J.-B. *Synth. Met.* **2012**, *162*, 1169; (c) Zhang, L.; Zhang, Q.; Yan, H.; Zhang, J.; Gu, J.; Zhang, H.; Guo, F. *Synth. Met.* **2009**, *159*, 2038.
 15. (a) Huang, P. H.; Shen, J.-Y.; Pu, S. C.; Wen, Y. S.; Wen, Y. S.; Lin, J. T.; Chou, P. T.; Yeh, M. C. P. *J. Mater. Chem.* **2006**, *16*, 850; (b) Lincker, F.; Kreher, D.; Attias, A.-J.; Do, J.; Kim, E.; Hapiot, P.; Lemaitre, N.; Geffroy, B.; Ulrich, G.; Ziessl, R. *Inorg. Chem.* **2010**, *49*, 3991.
 16. Achelle, S.; Malval, J. P.; Aloise, S.; Barsella, A.; Spangenberg, A.; Mager, L.; Akdas-Kılıç, H.; Fillaut, J. L.; Caro, B.; Robin-Le Guen, F. *ChemPhysChem* **2013**, *14*, 2725.
 17. (a) Lipunova, G. N.; Nosova, E. V.; Trashakhova, T. V.; Charushin, V. N. *Russ. Chem. Rev.* **2011**, *80*, 1115; (b) Vanden Eynde, J.-J.; Pascal, L.; Van Haverbeke, Y.; Dubois, P. *Synth. Commun.* **2001**, *31*, 3167.
 18. Pascal, L.; Vanden Eynde, J.-J.; Van Haverbeke, Y.; Dubois, P.; Michel, A.; Rant, U.; Zojer, E.; Leising, G.; Van Dorm, L. O.; Gruhn, N. E.; Cornil, J.; Brédas, J.-L. *Phys. Chem. B* **2002**, *106*, 6442.
 19. Reynolds, G. A.; Chen, C. H. *J. Org. Chem.* **1980**, *45*, 2453.
 20. Ba, F.; Robin-Le Guen, F.; Cabon, F.; Le Poul, P.; Golhen, S.; Le Poul, N.; Caro, B. *J. Organomet. Chem.* **2010**, *695*, 235.
 21. Hadad, C.; Achelle, S.; García-Martínez, J. C.; Rodríguez-López, J. *J. Org. Chem.* **2011**, *76*, 3837.
 22. (a) Scheibe, G.; Seiffert, W.; Hohlneicher, C.; Jutz, C.; Springer, H. J. *Tetrahedron Lett.* **1966**, *7*, 5053; (b) Blanchard-Desce, M.; Alain, V.; Bedworth, P. V.; Marder, S. R.; Fort, A.; Runser, C.; Barzoukas, M.; Lebus, S.; Wortmann, R. *Chem.—Eur. J.* **1997**, *3*, 1091.
 23. (a) Achelle, S.; Nouira, I.; Pfaffinger, B.; Ramondenc, Y.; Plé, N.; Rodríguez-López, J. *J. Org. Chem.* **2009**, *74*, 371; (b) Achelle, S.; Robin-le Guen. *Tetrahedron Lett.* **2013**, *54*, 4491; (c) Schmitt, V.; Moschel, S.; Detert, H. *Eur. J. Org. Chem.* **2013**, 5655; (d) Wink, C.; Detert, H. *J. Phys. Org. Chem.* **2013**, *26*, 144.
 24. Avó, J.; Parola, J.; Lima, J. C.; Pina, F.; Cunha-Silva, L. *J. Mater. Chem.* **2011**, *21*, 16628.
 25. Swamy, K. M. K.; Park, M. S.; Han, S. J.; Kim, S. K.; Kim, J. H.; Lee, C.; Bang, H.; Kim, Y.; Kim, S.-J.; Yoon, J. *Tetrahedron* **2005**, *61*, 10227.
 26. Akdas-Kılıç, H.; Roisnel, T.; Ledoux, I.; Le Bozec, H. *New J. Chem.* **2009**, *33*, 1470.
 27. Glinka, T. *Aldrichimica Acta* **1987**, *20*, 34.
 28. Reynolds, G. A.; van Allan, J. A. *J. Org. Chem.* **1969**, *34*, 2736.
 29. Crosby, G. A.; Demas, J. N. *J. Phys. Chem.* **1971**, *75*, 991.
 30. Frisch, M. J.; Trucks, G. W.; Schlegel, H. B.; Scuseria, G. E.; Robb, M. A.; Cheeseman, J. R.; Montgomery, J. A., Jr.; Vreven, T.; Kudin, K. N.; Burant, J. C.; Millam, J. M.; Iyengar, S. S.; Tomasi, J.; Barone, V.; Mennucci, B.; Cossi, M.; Scalmani, G.; Rega, N.; Petersson, G. A.; Nakatsuji, H.; Hada, M.; Ehara, M.; Toyota, K.; Fukuda, R.; Hasegawa, J.; Ishida, M.; Nakajima, T.; Honda, Y.; Kitao, O.; Nakai, H.; Klene, M.; Li, X.; Knox, J. E.; Hratchian, H. P.; Cross, J. B.; Adamo, C.; Jaramillo, J.; Gomperts, R.; Stratmann, R. E.; Yazev, O.; Austin, A. J.; Cammi, R.; Pomelli, C.; Ochterski, J. W.; Ayala, P. Y.; Morokuma, K.; Voth, G. A.; Salvador, P.; Dannenberg, J. J.; Zakrzewski, V. G.; Dapprich, S.; Daniels, A. D.; Strain, M. C.; Farkas, O.; Malick, D. K.; Rabuck, A. D.; Raghavachari, K.; Foresman, J. B.; Ortiz, J. V.; Cui, Q.; Baboul, A. G.; Clifford, S.; Cioslowski, J.; Stefanov, B. B.; Liu, G.; Liashenko, A.; Piskorz, P.; Komaromi, I.; Martin, R. L.; Fox, D. J.; Keith, T.; Al-Laham, M. A.; Peng, C. Y.; Nanayakkara, A.; Challacombe, M.; Gill, P. M. W.; Johnson, B.; Chen, W.; Wong, M. W.; Gonzalez, C.; Pople, J. A. *Gaussian 03, Revision B. 04*; Gaussian: Pittsburgh, PA, 2003.
 31. (a) Perdew, J. P.; Ernzerhof, M.; Burke, K. *J. Chem. Phys.* **1996**, *105*, 9982; (b) Perdew, J. P.; Burke, K.; Ernzerhof, M. *Phys. Rev. Lett.* **1996**, *77*, 3865; (c) Perdew, J. P.; Burke, K.; Ernzerhof, M. *Phys. Rev. Lett.* **1997**, *78*, 1396.
 32. (a) Dunning, T. H., Jr.; Hay, P. J. In *Methods of Electronic Structure Theory*; Schaeffer, H. F., Ed.; Plenum: New York, NY, 1977; (b) Hay, P. J.; Wadt, W. R. *J. Chem. Phys.* **1985**, *82*, 270; (c) Hay, P. J.; Wadt, W. R. *J. Chem. Phys.* **1985**, *82*, 284; (d) Hay, P. J.; Wadt, W. R. *J. Chem. Phys.* **1985**, *82*, 299.
 33. Schafer, A.; Horn, H.; Ahlrichs, R. *J. Chem. Phys.* **1992**, *97*, 2571.
 34. (a) Cossi, M.; Scalmani, G.; Rega, N.; Barone, V. *J. Chem. Phys.* **2002**, *117*, 43; (b) Barone, V.; Cossi, M.; Tomasi, J. *J. Chem. Phys.* **1997**, *107*, 3210.
 35. Glendening, E. D.; Badenhoop, J. K.; Reed, A. E.; Carpenter, J. E.; Bohmann, J. A.; Morales, C. M.; Weinhold, F. *Theoretical Chemistry Institute*; University of Wisconsin: Madison, WI, 2001; <http://www.chem.wisc.edu/~nbo5>.
 36. Gorelsky, S. I. AO Mix program, <http://www.sg-chem.net/>.
 37. Burke, K.; Gross, E. K. U. In *A Guided Tour of Time-dependent Density Functional Theory*; Joubert, D., Ed.; Density Functionals: Theory and Applications, (Lecture Notes in Physics); Springer: 1998; Vol. 500.
 38. (a) Sekino, H.; Bartlett, R. *J. J. Chem. Phys.* **1986**, *85*, 976; (b) Rice, J. E.; Handy, N. C. *Int. J. Quantum Chem.* **1992**, *43*, 91.
 39. Chai, J.-D.; Head-Gordon, M. *Phys. Chem. Chem. Phys.* **2008**, *10*, 6615.